

# Thermal Unfolding of Plastocyanin from the Mesophilic Cyanobacterium *Synechocystis* sp. PCC 6803 and Comparison with Its Thermophilic Counterpart from *Phormidium laminosum*<sup>†</sup>

Maria J. Feio,<sup>‡</sup> Antonio Díaz-Quintana, José A. Navarro, and Miguel A. De la Rosa\*

Instituto de Bioquímica Vegetal y Fotosíntesis, Universidad de Sevilla y Consejo Superior de Investigaciones Científicas, Centro de Investigaciones Científicas Isla de la Cartuja, Sevilla, Spain

Received November 11, 2005; Revised Manuscript Received February 21, 2006

**ABSTRACT:** The thermal unfolding of plastocyanin from the mesophilic cyanobacterium *Synechocystis* is described herein, and the results are compared with those obtained for the homologous thermophilic protein from *Phormidium laminosum*. The thermal unfolding is irreversible under all the conditions that were investigated. Plastocyanin from the thermophilic organism, both in the native state and in the apoprotein form, proved to be more thermostable than its mesophilic counterpart under all experimental conditions. *Synechocystis* reduced plastocyanin has been shown to be more stable than the oxidized species, both with respect to the required temperature for protein unfolding and with respect to the kinetics of the process. This behavior contrasts with that observed for *Phormidium* plastocyanin, in which the oxidized form is the more stable one. The unfolding pH dependence and kinetic studies indicate that around physiological pH, the most kinetically stable form is also the one more resistant to temperature variations, suggesting a close compromise between function and stability. Molecular dynamics simulations suggest that *Phormidium* and *Synechocystis* plastocyanins follow different unfolding pathways that affect different protein areas and which could be responsible for the observed dissimilar thermal resistance.

The molecular determinants of protein thermostability are extremely complex and not fully understood (1, 2). Several hypotheses have been advanced in terms of amino acid composition, namely, that (hyper)thermophilic proteins contain a reduced number of residues susceptible to deamination (asparagine and glutamine) and oxidation (cysteine and methionine) at high temperatures, more proline residues particularly rigidifying loops, and an increased level in aliphatic side chains resulting in better packing in hydrophobic cores (3). A slightly higher number of electrostatic interactions (salt bridges and hydrogen bonds), an increase in the fractional polar surface, a decrease in the number of loops and turns, and the stabilization of  $\alpha$ -helices (4, 5) are among the suggested structural features. However, the general consensus points to an increase in thermostability as a result of the additive effect of multiple and subtle changes in both structural elements and external interactions (3–5).

Plastocyanin (Pc)<sup>1</sup> is a small (~10.5 kDa) soluble copper protein, which functions as an electron shuttle between the cytochrome *b<sub>6</sub>f* complex and photosystem I (PS I) in oxygenic photosynthesis (6–10). Its 97–105 amino acids are arranged in a  $\beta$ -barrel formed by eight  $\beta$ -strands and a small  $\alpha$ -helix. Pc contains a single type I copper site that is coordinated in a distorted tetrahedral geometry (9, 11).

Earlier thermal stability studies of spinach Pc showed that the unfolding process was irreversible, following the general Lumry–Eyring scheme:



where N is the native protein, U is the reversible unfolded protein, and D is the irreversibly denatured protein (12). Recently, however, it has been demonstrated that the reduced spinach Pc under anaerobic conditions undergoes reversible thermal unfolding (13). A general mechanism for the irreversible thermal denaturation of Pc (applicable to all cupredoxins) was proposed on the basis of the covalent modification that occurs as a result of the copper-catalyzed oxidation of the metal-ligating cysteine sulfur under aerobic conditions (13, 14).

Previous studies have emphasized the high thermal stability of Pc from *Phormidium laminosum* (15), a filamentous thermophilic cyanobacterium that grows in hot springs at temperatures up to 60 °C (16). The thermal unfolding of

<sup>†</sup> This work was supported in part by research grants from the Human Potential Program, European Commission (The Transient RTN, HPRN-CT-1999-00095), the Spanish Ministry of Education and Science (BMC2003-0458), and the Andalusian Government (PAI-CVI-0198). M.J.F. was the recipient of an individual Marie-Curie Fellowship (QLK1-CT-2002-51483).

\* To whom correspondence should be addressed: Instituto de Bioquímica Vegetal y Fotosíntesis, Centro de Investigaciones Científicas Isla de la Cartuja, Universidad de Sevilla y CSIC, Américo Vespucio 49, 41092 Sevilla, Spain. Telephone: +(34) 954 489 506. Fax: +(34) 954 460 065. E-mail: marosa@us.es.

<sup>‡</sup> Current address: REQUIMTE, Departamento de Química, Faculdade de Ciências da Universidade do Porto, Rua do Campo Alegre, 687, 4000-069 Porto, Portugal.

<sup>1</sup> Abbreviations:  $k_{\text{obs}}$ , observed rate constant of protein thermal unfolding; MD, molecular dynamics; Pc, plastocyanin; PS I, photosystem I; rmsd, root-mean square deviation;  $T_M$ , midpoint temperature of the protein thermal transition.

this protein was irreversible under all the conditions that were studied, and this irreversibility did not appear to be associated with the presence of oxygen, observations that dismiss the proposed mechanism for the reversible unfolding of cupredoxins. The unfolding behavior of this Pc also contrasted with that of other Pcs previously described in that the oxidized species was more stable than the reduced one, in terms of both the thermodynamics and kinetics of the process.

This study is therefore an attempt to further clarify the reasons behind the unusual behavior exhibited by *P. laminosum* Pc by means of a comparison with its mesophilic counterpart from *Synechocystis* sp. PCC 6803, with regard to both the thermal resistance to unfolding and its dynamic properties at high temperatures.

## MATERIALS AND METHODS

**Protein Expression and Purification.** Recombinant *P. laminosum* Pc was overexpressed in *Escherichia coli* BL21-(DE3)pLysS transformed with the pET11Pc plasmid containing the *petE* coding region (courtesy of B. Schlär, University of Cambridge, Cambridge, U.K.) and purified from periplasmic extracts of harvested cells as described elsewhere (15). Recombinant *Synechocystis* sp. PCC 6803 Pc was overexpressed in *E. coli* and purified according to a previously described procedure (17), with an additional purification FPLC step (HiLoad 16/60 Sephadex-75 column, Pharmacia). A value of 2.5 for the  $A_{280}/A_{597}$  ratio was accepted for the pure protein (17). The protein concentration was determined spectrophotometrically using an absorption coefficient at 597 nm of  $4.5 \text{ mM}^{-1} \text{ cm}^{-1}$  for the oxidized form of Pc (17).

For experiments with oxidized Pc, samples were fully oxidized by addition of potassium ferricyanide (Sigma). Oxidant was eliminated by passing the sample through a PD10 Sephadex G-25M gel filtration column (Pharmacia). For experiments with reduced Pc, samples were treated with sodium ascorbate (Sigma) and the reducing agent was removed as described above. *P. laminosum* and *Synechocystis* apo-Pcs were prepared by adapting previously described procedures (18, 19). After incubation of 200  $\mu\text{L}$  of 1.5 mM protein with 200  $\mu\text{L}$  of 0.5 M Tris-HCl buffer (pH 7.2) containing 0.2 M KCN, the solution was first washed by ultrafiltration with 0.1 M Tris-HCl (pH 7.2) and 50 mM KCN buffer and finally extensively washed with 10 mM phosphate (pH 6.5) to remove KCN. The apo-Pc concentration was determined using an estimated absorption coefficient at 278 nm of  $10 \text{ mM}^{-1} \text{ cm}^{-1}$  (ProtParam tool in the ExPASy server).

**Fluorescence Spectroscopy.** Fluorescence measurements were recorded as previously described (15). Samples contained 25  $\mu\text{M}$  Pc in 10 mM sodium citrate buffer adjusted to pH values ranging from 4.5 to 7.5. Reduced Pc samples were studied in the presence of equimolar concentrations of sodium ascorbate to prevent auto-oxidation of the protein throughout the experiment. Temperature changes during thermal denaturation of Pc were controlled and monitored as previously described (15). A scan rate of  $1^\circ\text{C}/\text{min}$  was used between 25 and  $95^\circ\text{C}$ . Data were corrected for the sloping of the baselines for the folded and unfolded protein forms and normalized to calculate the fraction of folded protein. Curves were fitted to a two-state equilibrium mechanism for protein unfolding to estimate the  $T_M$  values

(15, 20). The kinetic studies were carried out under the same conditions as described previously (15). Experiments conducted with different protein concentrations ranging between 5 and 50  $\mu\text{M}$  showed that there was no concentration dependence of the unfolding experimental data within the range that was tested. Equivalent experiments were also conducted under anaerobic conditions, using a sealed quartz cell and solutions thoroughly degassed under an argon flow, to test the effect of anaerobiosis on the unfolding process and its reversibility.

**Molecular Dynamics.** Molecular dynamics (MD) calculations were performed on the structures of *P. laminosum* (PDB entry 1BAW) and *Synechocystis* (PDB entry 1PCS) Pcs at 298, 363, and 495 K, using AMBER version 4.1 (21) under the AMBER force field (22) in a RC10000 SGI workstation. All simulations were performed under periodic boundary conditions using a nonbonded cutoff of 8 Å and a constant dielectric function. Copper force field parameters were those developed by Ungar et al. for Cu(II) (23). Crystallographic water molecules (75 and 13 for *Synechocystis* and *P. laminosum* Pc, respectively) and counterions (2 and 4, respectively) were added with the EDIT module of AMBER version 4.1. Both proteins were then fully solvated with a cube of TIP3P water molecules (5540 and 5372 for *Synechocystis* and *P. laminosum* Pc, respectively) (24) using the same module. Protein side chains were then energy-minimized (250 steepest descent and 750 conjugate gradient steps) down to an rms energy gradient of  $0.125 \text{ kJ mol}^{-1} \text{ Å}^{-1}$ , using the SANDER module of AMBER (21). After that, solvent and counterions were submitted to 500 steps of steepest descent minimization and then submitted to 5 ps of NTP-MD using isotropic molecule position scaling and a pressure relaxation time of 0.2 ps at 298 K. The temperature was regulated using Berendsen's heat bath algorithm (25), with a coupling time constant of 0.2 ps. For each protein, the whole system was then energy minimized and submitted to canonical MD at 298 K for 1 ns, using 2 fs integration time steps. The SHAKE algorithm (26) was used only to constrain bonds involving hydrogen atoms. MD calculations at 363 and 495 K were carried out using the snapshots at 200 ps trajectories as starting points. For this purpose, the water box was re-equilibrated by NTP-MD as before. Integration intervals were reduced to 0.5 fs to avoid excessive heating.

Trajectories were processed with the CARNAL module of AMBER. Secondary structure analysis was performed with the algorithm of Kabsch and Sander, as implemented in MOLMOL (27, 28).

## RESULTS AND DISCUSSION

**Thermal Unfolding of *Synechocystis* sp. PCC 6803 Plastocyanin.** In a previous study, fluorescence spectroscopy was used to investigate the factors influencing the thermal unfolding of Pc from the thermophilic organism *P. laminosum*, and the reliability of this approach was confirmed by EPR and NMR spectroscopies (15). Here we have studied the thermal unfolding of Pc from the mesophilic cyanobacterium *Synechocystis* sp. PCC 6803, to obtain new information about the factors that confer stability to proteins under extreme conditions. The fluorescence emission spectra of the oxidized and reduced forms of *Synechocystis* Pc (not shown)

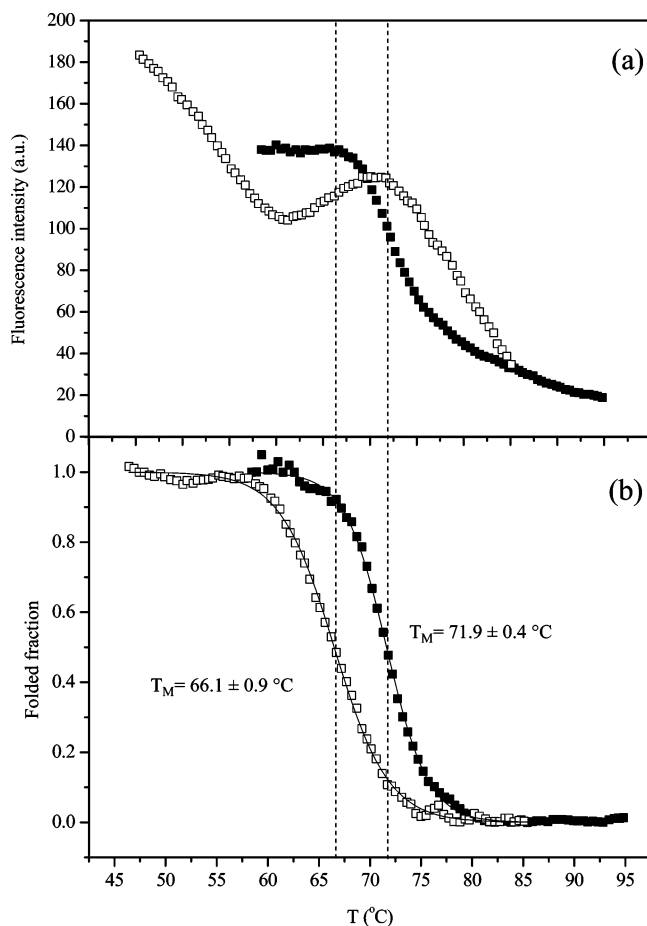


FIGURE 1: (a) Thermal unfolding of the oxidized ( $\square$ ) and reduced ( $\blacksquare$ ) *Synechocystis* plastocyanin followed by the fluorescence emission at 325 nm under aerobic conditions. Samples containing 25  $\mu$ M protein in 10 mM citrate buffer (pH 5.5) were subjected to a temperature gradient of 1  $^{\circ}$ C/min. (b) Normalized thermal unfolding curves (see Materials and Methods for details).

do not differ significantly from those previously published for *P. laminosum* Pc (15). The fluorescence emission spectra are dominated by a band with a maximum around 325 nm, which mainly arises from the  $\pi$ – $\pi^*$  transitions in the indole ring of the unique tryptophan residue when surrounded by the relatively rigid protein structure and other apolar amino acid side chains (29). As the protein unfolds, both oxidized and reduced forms exhibit a red-shifted spectrum, with a maximum around 350 nm and a lower quantum yield that results from aqueous solvent quenching.

Typical thermal unfolding curves for both the oxidized and reduced forms of *Synechocystis* Pc under aerobic conditions at pH 5.5 can be seen in Figure 1. As previously described (15), the curves could be adequately adjusted to a two-state model for protein unfolding, assuming that the irreversible step is much slower than the initial reversible process and takes place mainly at temperatures above  $T_M$  (20, 30). This way, the data were normalized to describe the fraction of folded protein and revealed a significant difference in the  $T_M$  values obtained for the oxidized and reduced forms of the protein, 66.1 and 71.9  $^{\circ}$ C, respectively (Figure 1b). The  $T_M$  value obtained for the oxidized form of the protein is higher than the value previously reported, 57.7  $^{\circ}$ C at pH 7.5 (31), although a closer value (ca. 62  $^{\circ}$ C) was obtained at neutral pH (Figure 2a). However, the

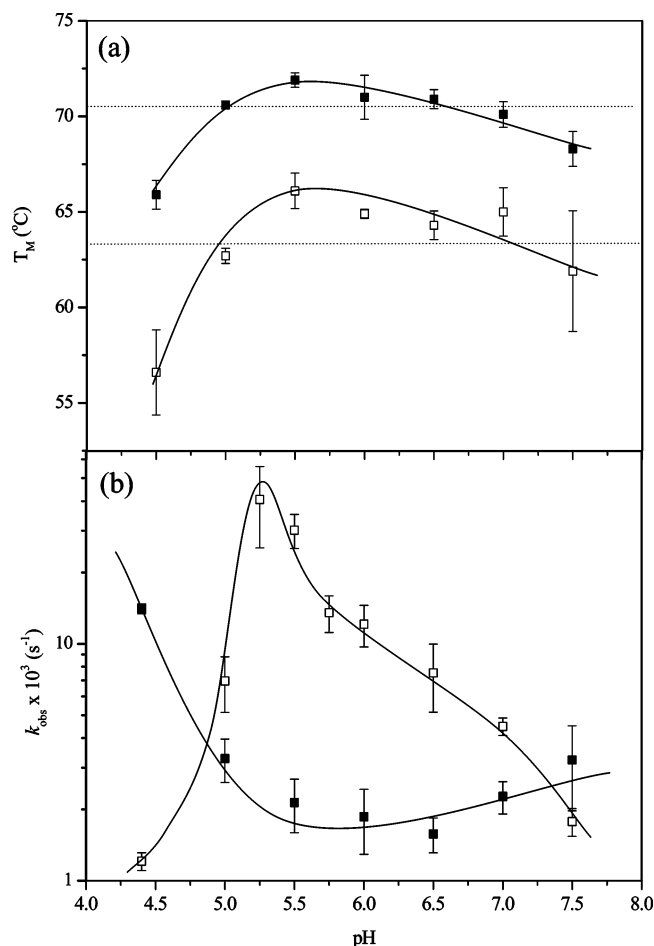


FIGURE 2: pH dependence of (a) the midpoint unfolding temperature ( $T_M$ ) and (b) the observed rate constant ( $k_{\text{obs}}$ ) for the unfolding kinetics for the oxidized ( $\square$ ) and reduced ( $\blacksquare$ ) forms of *Synechocystis* plastocyanin. The kinetic curves were obtained at 63 and 71  $^{\circ}$ C, respectively (see the text for full details). Error bars represent standard deviation values based on at least three independent experiments and are taken into account in the determination of the most probable fit.

observed differences are likely due to methodological differences in the temperature gradients used, as previously reported (15): a continuous temperature gradient (this work) against a step gradient with equilibration times between increments (31). Previous reports (15) assigned to *P. laminosum* Pc  $T_M$  values (76.4 and 83.1  $^{\circ}$ C for reduced and oxidized Pc, respectively) much higher than those reported here for *Synechocystis* Pc under the same experimental conditions. This experimental evidence corroborates our predictions given the known thermophilic nature of *P. laminosum*. In addition, as previously reported for *P. laminosum* (15), all the studies conducted with *Synechocystis* Pc also showed consistent results with regard to the irreversibility of the unfolding process, namely, trials conducted under anaerobic conditions (see Materials and Methods for details). Ultimately, the intrinsic irreversibility of the unfolding prevents the direct equilibrium thermodynamic analysis of the process.

Unlike the unfolding curves reported for *P. laminosum* Pc (15), which were relatively complex and showed an earlier  $T_M$  value, the curves obtained for *Synechocystis* Pc exhibited no such transition. The shape of the curves for the magnitude of fluorescence change varies with the oxidation state of the



copper center (Figure 1a), thus yielding normalized curves with different slopes (Figure 1b). The experimental conditions were constant in all experiments, so the reason for such a difference is not known; however, it could be an effect of the irreversible nature of protein unfolding or a reflection of the different  $\Delta H$  values for the unfolding of oxidized and reduced forms. A more detailed thermodynamic analysis would be required to make this point clearer, but as stated above, this is hindered by the observed denaturation process.

From the results shown in Figure 2a, it is clear that the reduced form of *Synechocystis* Pc is consistently more thermostable than its oxidized form throughout the whole range of pH values that was studied. Remarkably, it can be seen that the pH dependence appears to have a maximum of stability, for both the oxidized and reduced forms, around pH 5.5, the pI described for this protein (17), and around the physiological pH value assumed for the thylakoid lumen. An identical behavior has been described for *P. laminosum* Pc (15), supporting the suggestion that maximum protein thermostability is attained around the protein's pI and its operative pH, in a close compromise between functional efficiency and stability.

**Kinetics of the Thermal Unfolding in *Synechocystis*.** The thermal unfolding in *Synechocystis* Pc was followed at different pH values as a function of time. All experiments were conducted at a constant temperature, 63 and 71 °C for the oxidized and reduced forms of Pc, respectively. These values correspond to the average of the  $T_M$  values determined within the pH range that was studied (Figure 2a, dashed lines).

Typical unfolding curves could be fitted to a single-exponential decay (data not shown), and the values of the observed rate constants ( $k_{\text{obs}}$ ) were calculated (Figure 2b). There are drastic differences in the kinetic behavior presented by the oxidized and reduced forms of *Synechocystis* Pc. The  $k_{\text{obs}}$  values determined for the reduced form show a much less pronounced dependence upon pH, with a marked decrease between pH 4.5 and 5.5, but almost no variation for higher pH values (Figure 2b). A parallel can be drawn between this  $k_{\text{obs}}$  minimum above pH  $\sim 5$ , associated with the highest kinetic stability, and the conditions under which the protein showed the highest thermodynamic stability (Figure 2a). A similar kinetic pattern with a stability maximum at pH 5.6 has been reported for the oxidized form of *P. laminosum* Pc, whereas the thermal unfolding of the reduced species was too fast to be measured (15). However, the kinetic behavior of the oxidized *Synechocystis* Pc displays a much tighter pH dependence, showing a minimum of kinetic stability under the same conditions (pH 5–5.5) (Figure 2b). These data, considered along with the thermodynamic data herein described, could indicate some control or regulation mechanism that favors the reduced form of the mesophilic Pc at high temperatures. Hence, the behavior observed could be associated with a stress response, thus ensuring that only one of the protein forms, the more thermostable, is maintained at high temperatures, destabilizing the excess of the redox form not able to perform its normal function and preventing unspecific electron transfer reactions.

**Apoplastocyanin Studies.** The increased thermostability exhibited by the reduced form of *Synechocystis* Pc is in tune with the results previously described for spinach Pc (13, 32)

but is in clear contrast with those reported for *P. laminosum* Pc, for which the oxidized species has proven to be the more stable one, with respect to both the required temperature for unfolding and the kinetics of the process (15). In this sense, as reduced Pc is spontaneously converted in vitro to the oxidized species at high temperatures, *P. laminosum* Pc's unusual behavior could be understood as a reflection of its thermophilic nature when compared to mesophilic prokaryotic and eukaryotic Pcs.

Previous studies of the unfolding of the related bacterial cupredoxins rusticyanin and azurin have also revealed oxidized species that were more stable (33, 34). This differential stability has been explained in terms of different conformations for the oxidized and reduced protein in the unfolded state, leading to a higher affinity of the apoprotein for the copper(II) atom and thus favoring the Cu(II)Pc folded form (33, 34). In addition, the possibility that some of the significant stability differences observed between the Pc redox forms could be associated with modifications in the native metal center geometry cannot be discarded. Pc global structure is almost identical in its two redox forms and in different organisms (11, 35–37). However, there are some small differences in all structures that affect mainly the geometry of the metal center (18, 35, 36, 38). In particular, differences in  $^1\text{H}$  and  $^{15}\text{N}$  chemical shifts detected with *Synechococcus* sp. PCC 7942 Pc suggest that small structural rearrangements, localized in the northern loops close to the copper atom, may occur with the redox change (38). Recently, an unfolding study with amicyanin has confirmed such suggestions by showing that the thermal stability of the protein is dictated mainly by the presence or absence of the copper atom and its ligand geometry, but not by its redox state (39).

To investigate whether the higher thermostability of *P. laminosum* Pc could be ascribed to differences in the primary structure, we have determined the  $T_M$  values for apo-Pc from both *P. laminosum* and *Synechocystis* under standard conditions at pH 5.5 to be 55.6 and 47.1 °C, respectively (not shown). From the results obtained (Figure 3), it is clear that the native forms of both proteins exhibit increases in  $T_M$  as high as 20–25 °C when compared with those of the apo forms, strongly suggesting that the metal center has a key role in the thermal stabilization of the protein, as previously reported for other cupredoxins (40). Therefore, small modifications to the center structure could promote important changes to the overall stability of Pc. In addition, *P. laminosum* apo-Pc has been shown to be more thermostable than its mesophilic counterpart ( $\Delta T_M = 8.5$  °C), supporting once more the evidence of an optimization of stability in agreement with the thermophilic nature of the organism.

**Ionic Strength Dependence.** The ionic strength inside the thylakoid is considered to be 0.2–0.3 M. Thus, we have undertaken a comparative study of the effect of the ionic strength upon the  $T_M$  values, both in *P. laminosum* and in *Synechocystis* Pcs, to gain insight into the factors that govern the thermostability under more physiological conditions. All experiments were carried out with the oxidized form of the proteins at pH 5.5. It can be seen that both Pcs are differently affected by the addition of salt (Figure 4), although in both cases the higher the quantity of salt present, the stronger the destabilizing effect on the unfolding process. Nevertheless, this destabilizing effect is much more pronounced in the case

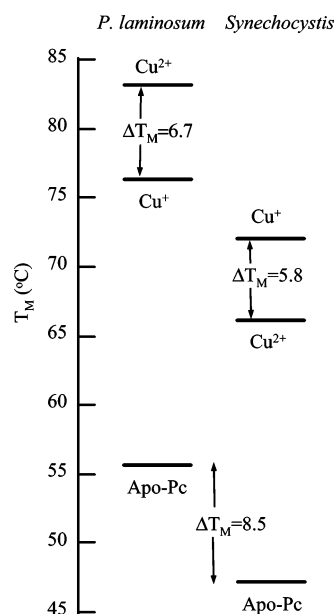


FIGURE 3: Diagram showing the mean midpoint unfolding temperature ( $T_M$ ) values for the different redox species of *P. laminosum* and *Synechocystis* Pc and its apoproteins.

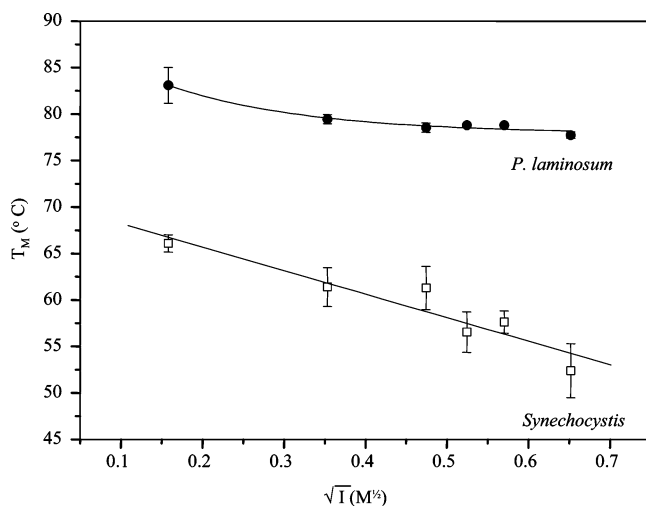


FIGURE 4: Ionic strength dependence of the midpoint unfolding temperature ( $T_M$ ) for the oxidized forms of *P. laminosum* and *Synechocystis* plastocyanins. The experimental conditions were as stated in Figure 1. Ionic strength variations were attained by addition of NaCl. Error bars represent standard deviation values based on at least five independent replicates and are taken into account in the determination of the most probable fit.

of *Synechocystis* Pc. The different effect of ionic strength highlights considerable differences in terms of the molecular interactions at the surface level relevant in the stabilization of the protein. Thus, in *P. laminosum* Pc, electrostatic interactions appear to be less important in the stabilization process than in the case of *Synechocystis* Pc. Electrostatic interactions are considered to be more sensitive to increases in temperature, and accordingly, protein stabilization mainly based on hydrophobic interactions could be a likely strategy in proteins from thermophilic organisms. Coincidentally, the electrostatic interactions also seem to play a lesser role in the complex formation process between *P. laminosum* Pc and both cytochrome *f* and PS I, in contrast to other systems, an observation that has also been linked to the thermophilic nature of the species (41).

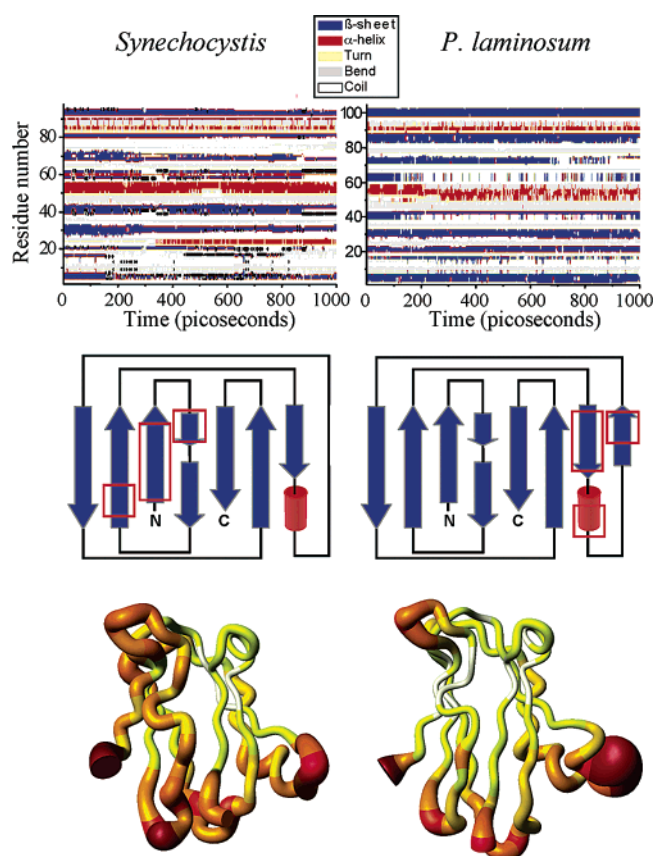


FIGURE 5: Molecular dynamics analysis of plastocyanin unfolding. (a) Secondary structures of *Synechocystis* and *P. laminosum* plastocyanin along their 363 K trajectories. See Materials and Methods for further details. (b) Topological diagrams of *Synechocystis* and *P. laminosum* plastocyanin showing (red rectangles) the secondary elements that are first perturbed along their respective trajectories. (c) Representation of *Synechocystis* and *P. laminosum* plastocyanin showing the regions with higher mobilities. Both plastocyanins are oriented with their electrostatic patches, or east areas, pointing to the right. The bond diameter is proportional to  $B$  factors calculated from the rmsd from 250 snapshots along each MD trajectory with respect to their mean structure. Colors correspond to different  $B$  factors: white,  $B < 1.00$  Å; yellow,  $1.00$  Å  $< B < 1.25$  Å; light orange,  $1.25$  Å  $< B < 1.50$  Å; orange,  $1.50$  Å  $< B < 1.75$  Å; red,  $1.75$  Å  $< B < 2.0$  Å; and brown,  $B \geq 2.00$  Å.

**Molecular Dynamics.** The different unfolding behaviors of *P. laminosum* and *Synechocystis* Pc, in terms of both the thermodynamics and the kinetics of the denaturation process, indicate the occurrence of differences in the transition states between the folded and unfolded forms of these proteins, mainly affecting their respective oxidized forms (Figure 3). To clarify this possibility, short MD simulations have been performed on both oxidized proteins at 298 (not shown), 363 (Figure 5), and 495 K (not shown); the two latter are temperatures above the  $T_M$  values determined for both proteins. The rmsds of backbone atoms after 1 ns at 298 K, with respect to the starting energy-minimized structures, were 1.3 and 1.1 Å for *Synechocystis* and *P. laminosum* Pcs, respectively. At 363 K, on the other hand, the structures evolved along their trajectories, and their rmsds (with respect to the starting energy-minimized structures) after 1 ns were 2.7 and 2.2 Å for *Synechocystis* and *P. laminosum* Pcs, respectively, at the end of the trajectory (not shown). That is, *Synechocystis* Pc suffers larger structural changes than

the protein from *P. lamosum*, in agreement with the lower stability of the former protein.

It is worth noting that the structural changes along the trajectories at 363 K are not spread along the protein structure, but they are concentrated in defined regions which are different in both Pcs. Figure 5 shows that upon heating, *Synechocystis* Pc experiences a destabilization of the first and second  $\beta$ -strands, leading to a further loss of secondary structure at the third  $\beta$ -strand, with a concomitant increase in the mobility of this entire protein region. On the other hand, the same region is stable in *P. lamosum* Pc (Figure 5). Remarkably, in *P. lamosum* Pc, a phenylalanine residue at position 3 (alanine in *Synechocystis*) keeps van der Waals contacts with the side chains of Val-21 and Val-23 (Thr-23 in *Synechocystis*) along the trajectory, despite the high rmsd of the two first residues at the N-terminus, thus stabilizing this protein region. However, *P. lamosum* Pc exhibits a lower stability around the east electrostatic patch, affecting  $\beta$ -strands 5 and 6 and the short  $\alpha$ -helix region, as inferred from trajectories at both 363 (Figure 5) and 495 K (not shown). Although the two  $\beta$ -strands are slightly affected in the trajectories of *Synechocystis* Pc (they both disappear simultaneously during some intervals), the  $\alpha$ -helix remains stable. Interestingly, the known structures of *P. lamosum* and *Synechocystis* Pc reveal that they both differ in the hydrogen bonding pattern between strands 6 and 7.

With regard to the dynamics of the  $\beta$ -barrel at the east patch, not only is the time course quite different from one protein to another but there are also several distinct features in *P. lamosum* Pc as compared with the protein from *Synechocystis*. First, there is a three-residue insertion (positions 47–49) that could confer a higher flexibility to this region in *P. lamosum* Pc, although such an increase in flexibility may be in part compensated by the presence of a proline residue at position 49. Second, all native contacts in this region (including nonconserved residues) are lost after 1 ns at 495 K in *P. lamosum* Pc, but not in *Synechocystis* Pc. Third, *P. lamosum* Pc contains more charged residues at this east patch, thus imposing certain restraint on the structure.

Thus, thermal unfolding in *P. lamosum* and *Synechocystis* Pcs follows different pathways affecting different protein areas, which can justify the dissimilar thermal resistance of both proteins.

In conclusion, amino acid sequence comparison of *P. lamosum* and *Synechocystis* Pcs reveals 61% homology (42). Despite this considerable degree of homology, these two proteins exhibit significant differences with regard to their thermal unfolding behavior and molecular dynamics. It became clear from our study that Pc from the thermophilic organism, both in the native state and in the apoprotein form, is more thermostable than its counterpart from the mesophilic cyanobacterium under all experimental conditions that were tested. Like other cupredoxins that have been studied, *Synechocystis* Pc exhibited higher thermostability in the reduced form than in the oxidized one, a behavior that is in clear contrast with the behavior exhibited by *P. lamosum* Pc. This phenomenon is likely to be related to the temperature-resistant nature of the organism in a control process that seems to favor one redox form over the other. This hypothesis is supported by the kinetic studies of thermal unfolding given that, around physiological pH, the most

kinetically stable form is also the more resistant to temperature variations. This study provides a further example of the compromise between functional efficiency and stability previously suggested.

## ACKNOWLEDGMENT

We thank Dr. Manuel Hervás (IBVF) for the helpful discussions and for critically reading the manuscript, and Dr. Irene Díaz-Moreno for her technical guidance in preparing the apoplastocyanin samples.

## REFERENCES

1. Szilagyi, A., and Zavodszky, P. (2000) Structural differences between mesophilic, moderately thermophilic and extremely thermophilic protein subunits: Results of a comprehensive survey, *Structure* 8, 493–504.
2. Das, R., and Gerstein, M. (2000) The stability of thermophilic proteins: A study based on comprehensive genome comparison, *Funct. Integr. Genomics* 1, 76–88.
3. Macedo-Ribeiro, S., Martins, B. M., Pereira, P. J. B., Buse, G., Huber, R., and Soulimane, T. (2001) New insights into the thermostability of bacterial ferredoxins: High-resolution crystal structure of the seven-iron ferredoxin from *Thermus thermophilus*, *J. Biol. Inorg. Chem.* 6, 663–674.
4. Kumar, S., and Nussinov, R. (2001) How do thermophilic proteins deal with heat? *Cell. Mol. Life Sci.* 58, 1216–1233.
5. Vogt, G., Woell, S., and Argos, P. (1997) Protein thermal stability, hydrogen bonds, and ion pairs, *J. Mol. Biol.* 269, 631–643.
6. Sigfridsson, K. (1998) Plastocyanin, an electron-transfer protein, *Photosynth. Res.* 57, 1–28.
7. Hope, A. B. (2000) Electron transfers amongst cytochrome *f*, plastocyanin and photosystem I: Kinetics and mechanisms, *Biochim. Biophys. Acta* 1456, 5–26.
8. Hervás, M., Navarro, J. A., and De La Rosa, M. A. (2003) Electron transfer between membrane complexes and soluble proteins in photosynthesis, *Acc. Chem. Res.* 36, 798–805.
9. Bond, C. S., Bendall, D. S., Freeman, H. C., Guss, J. M., Howe, C. J., Wagner, M. J., and Wilce, M. C. J. (1999) The structure of plastocyanin from the cyanobacterium *Phormidium lamosum*, *Acta Crystallogr. D* 55, 414–421.
10. Diaz-Quintana, A., Navarro, J. A., Hervás, M., Molina-Heredia, F. P., De la Cerda, B., and De la Rosa, M. A. (2003) A comparative structural and functional analysis of cyanobacterial plastocyanin and cytochrome *c<sub>6</sub>* as alternative electron donors to Photosystem I: Photosystem I reduction in cyanobacteria, *Photosynth. Res.* 75, 97–110.
11. Bertini, I., Ciurli, S., Dikiy, A., Fernandez, C. O., Luchinat, C., Safarov, N., Shumilin, S., and Vila, A. J. (2001) The first solution structure of a paramagnetic copper(II) protein: The case of oxidized plastocyanin from the cyanobacterium *Synechocystis* PCC 6803, *J. Am. Chem. Soc.* 123, 2405–2413.
12. Milardi, D., La Rosa, C., Grasso, D., Guzzi, R., Sportelli, L., and Fini, C. (1998) Thermodynamics and kinetics of the thermal unfolding of plastocyanin, *Eur. Biophys. J.* 27, 273–282.
13. Sandberg, A., Harrison, D. J., and Karlsson, B. G. (2003) Thermal denaturation of spinach plastocyanin: Effect of copper site oxidation state and molecular oxygen, *Biochemistry* 42, 10301–10310.
14. Sandberg, A., Leckner, J., Shi, Y., Schwarz, F. P., and Karlsson, B. G. (2002) Effects of metal ligation and oxygen on the reversibility of the thermal denaturation of *Pseudomonas aeruginosa* azurin, *Biochemistry* 41, 1060–1069.
15. Feio, M. J., Navarro, J. A., Teixeira, M. S., Harrison, D., Karlsson, B. G., and De la Rosa, M. A. (2004) A thermal unfolding study of plastocyanin from the thermophilic cyanobacterium *Phormidium lamosum*, *Biochemistry* 43, 14784–14791.
16. Castenholz, R. W. (1970) Laboratory culture of thermophilic cyanophytes, *Schweiz. Z. Hydrol.* 32, 538–551.
17. Hervás, M., Navarro, F., Navarro, J. A., Chavez, S., Diaz, A., Florencio, F. J., and De la Rosa, M. A. (1993) *Synechocystis*-6803 plastocyanin isolated from both the cyanobacterium and *Escherichia coli* transformed-cells are identical, *FEBS Lett.* 319, 257–260.
18. Danielsen, E., Scheller, H. V., Bauer, R., Hemmingsen, L., Bjerrum, M. J., and Hansson, O. (1999) Plastocyanin binding to



- photosystem I as a function of the charge state of the metal ion: Effect of metal site conformation, *Biochemistry* 38, 11531–11540.
19. Ubbink, M., Lian, L. Y., Modi, S., Evans, P. A., and Bendall, D. S. (1996) Analysis of the <sup>1</sup>H-NMR chemical shifts of Cu(I)-, Cu(II)- and Cd-substituted pea plastocyanin: Metal-dependent differences in the hydrogen-bond network around the copper site, *Eur. J. Biochem.* 242, 132–147.
  20. Privalov, P. L. (1979) Stability of proteins: Small globular proteins, *Adv. Protein Chem.* 33, 167–241.
  21. Pearlman, D. A., Case, D. A., Cadwell, G. C., Siebel, G. L., Singh, U. C., Weiner, P., and Kollman, P. A. (1995) AMBER, version 4.1, University of California, San Francisco.
  22. Cornell, W. D., Cieplak, P., Bayly, C. I., Gould, I. R., Merz, K. M., Ferguson, D. M., Spellmeyer, D. C., Fox, T., Caldwell, J. W., and Kollman, P. A. (1995) A second generation force-field for the simulation of proteins, nucleic-acids, and organic-molecules, *J. Am. Chem. Soc.* 117, 5179–5197.
  23. Ungar, L. W., Scherer, N. F., and Voth, G. A. (1997) Classical molecular dynamics simulation of the photoinduced electron-transfer dynamics of plastocyanin, *Biophys. J.* 52, 5–17.
  24. Jorgensen, W. L., Chandrasekhar, J., Madura, R. J. D., Impey, W., and Klein, M. L. (1983) Comparison of simple potential functions for simulating liquid water, *J. Chem. Phys.* 79, 926–935.
  25. Berendsen, H. J. C., Postma, J. P. M., Vangunsteren, W. F., Dinola, A., and Haak, J. R. (1984) Molecular dynamics with coupling to an external bath, *J. Chem. Phys.* 81, 3684–3690.
  26. Ryckaert, J. P., Ciccotti, G., and Berendsen, H. J. C. (1977) Numerical-integration of Cartesian equations of motion of a system with constraints: Molecular dynamics of N-alkanes, *J. Comput. Phys.* 23, 327–341.
  27. Kabsch, W., and Sander, C. (1983) Dictionary of protein secondary structure: Pattern-recognition of hydrogen-bonded and geometrical features, *Biopolymers* 22, 2577–2637.
  28. Koradi, R., Billeter, M., and Wuthrich, K. (1996) MOLMOL: A program for display and analysis of macromolecular structures, *J. Mol. Graphics* 14, 51–55.
  29. Eftink, M. R. (1998) The use of fluorescence methods to monitor unfolding transitions in proteins, *Biochemistry (Moscow)* 63, 276–284.
  30. Milardi, D., La Rosa, C., and Grasso, D. (1994) Extended theoretical-analysis of irreversible protein thermal unfolding, *Biophys. Chem.* 52, 183–189.
  31. Balme, A., Hervás, M., Campos, L. A., Sancho, J., De la Rosa, M. A., and Navarro, J. A. (2001) A comparative study of the thermal stability of plastocyanin, cytochrome *c*<sub>6</sub> and Photosystem I in thermophilic and mesophilic cyanobacteria, *Photosynth. Res.* 70, 281–289.
  32. Gross, E. L., Draheim, J. E., Curtiss, A. S., Crombie, B., Scheffer, A., Pan, B., Chiang, C., and Lopez, A. (1992) Thermal denaturation of plastocyanin: The effect of oxidation state, reductants, and anaerobicity, *Arch. Biochem. Biophys.* 298, 413–419.
  33. Alcaraz, L. A., and Donaire, A. (2004) Unfolding process of rusticyanin: Evidence of protein aggregation, *Eur. J. Biochem.* 271, 4284–4292.
  34. Leckner, J., Wittung, P., Bonander, N., Karlsson, B. G., and Malmstrom, B. G. (1997) The effect of redox state on the folding free energy of azurin, *J. Biol. Inorg. Chem.* 2, 368–371.
  35. Guss, J. M., and Freeman, H. C. (1983) Structure of oxidized poplar plastocyanin at 1.6 Å resolution, *J. Mol. Biol.* 169, 521–563.
  36. Guss, J. M., Harrowell, P. R., Murata, M., Norris, V. A., and Freeman, H. C. (1986) Crystal-structure analyses of reduced (CuI) poplar plastocyanin at 6 pH values, *J. Mol. Biol.* 192, 361–387.
  37. Inoue, T., Sugawara, H., Hamanaka, S., Tsukui, H., Suzuki, E., Kohzuma, T., and Kai, Y. (1999) Crystal structure determinations of oxidized and reduced plastocyanin from the cyanobacterium *Synechococcus* sp. PCC 7942, *Biochemistry* 38, 6063–6069.
  38. Bertini, I., Bryant, D. A., Ciurli, S., Dikiy, A., Fernandez, C. O., Luchinat, C., Safarov, N., Vila, A. J., and Zhao, J. D. (2001) Backbone dynamics of plastocyanin in both oxidation states: Solution structure of the reduced form and comparison with the oxidized state, *J. Biol. Chem.* 276, 47217–47226.
  39. Ma, J. K., Bishop, G. R., and Davidson, V. L. (2005) The ligand geometry of copper determines the stability of amicyanin, *Arch. Biochem. Biophys.* 444, 27–33.
  40. Pozdnyakova, I., Guidry, J., and Wittung-Stafshede, P. (2001) Copper stabilizes azurin by decreasing the unfolding rate, *Arch. Biochem. Biophys.* 390, 146–148.
  41. Diaz-Moreno, I., Diaz-Quintana, A., De la Rosa, M. A., Crowley, P. B., and Ubbink, M. (2005) Different modes of interaction in cyanobacterial complexes of plastocyanin and cytochrome *f*, *Biochemistry* 44, 3176–3183.
  42. Varley, J. P. A., Moehle, J. J., Manasse, R. S., Bendall, D. S., and Howe, C. J. (1995) Characterization of plastocyanin from the cyanobacterium *Phormidium laminosum* copper-inducible expression and SecA-dependent targeting in *Escherichia coli*, *Plant Mol. Biol.* 27, 179–190.

BI052312Q